DALTON

Equilibria and rates of olefin substitution in zerovalent palladium complexes containing a 2-pyridylmethanimine ligand†

Luciano Canovese,*[a] Fabiano Visentin,[a] Paolo Uguagliati[a] and Bruno Crociani[b]

[a] *Dipartimento di Chimica, Università di Venezia, Venice, Italy*
[b] *Dipartimento di Scienze e Tecnologie Chimiche, II Università di Roma, Rome, Italy*

Equilibrium constants K_e have been determined for the olefin susbtitution in palladium(0) α-diimine olefin (ol) complexes [Pd(η^2-ol)(L–L)] by ol′ in chloroform [L–L = 2-NC_5H_4CH=NC_6H_4OMe-4; ol = dimethyl fumarate (dmf), ol′ = acrylonitrile (an), 1-chloro-1-cyanoethylene, 1,4-naphthoquinone (nq), tetramethyl ethylenetetracarboxylate (tmetc), fumaronitrile (fn) or maleic anhydride (ma); ol = nq, ol′ = tmetc, fn or ma]. The substitution equilibria are rapidly established except when ol = dmf, nq, ol′ = tmetc and were studied by UV/VIS and ^{1}H NMR spectrometry. The K_e values increase with increasing electron affinity of the entering activated olefin. The kinetics of slow approach to equilibrium were monitored by UV/VIS techniques at various temperatures. When ol = dmf, ol′ = tmetc, only the second-order rate constant k_2 for the forward step could be measured with sufficient accuracy, whereas for ol = nq, ol′ = tmetc the constants for both the forward (k_2) and the reverse (k_{-2}) steps were determined. Activation parameters indicate an essentially associative mechanism for these paths.

2-Pyridylmethanimines, 2-NC_5H_4CH=NR, represent a quite interesting and versatile class of bidentate nitrogen donors of the α-diimine type which have been employed as ligands in a variety of transition-metal complexes. Their ligating properties can be conveniently varied by a suitable choice of substituents R at the imino nitrogen and/or at the pyridine C(6) carbon.[1] Furthermore, related compounds with palladated imino carbons, such as 2-$NC_5H_4C(R')$ = NR {R′ = *trans*-PdL_2Cl (L = tertiary phosphine) or PdCl(dppe) [dppe = 1,2-bis(diphenylphosphino)ethane]} were also reported.[2]

We have been carrying out a systematic investigation of the reactivity of the cationic complexes [Pd(η^3-allyl)(L–L)]$^+$ (L–L = 2-pyridylmethanimine) towards nucleophilic attacks by the tetraphenylborate anion[3] or secondary amines[4–6] in the presence of activated olefins. These reactions led to phenylation or amination of the allyl moiety and concomitant formation of palladium(0) complexes [Pd(η^2-olefin)(L–L)]. We have also proposed a mechanism for the reverse of the amination reaction, *i.e.* the oxidative allyl transfer from allylammonium cations to [Pd(η^2-olefin)(L–L)], which results in the formation of [Pd(η^3-allyl)(L–L)]$^+$ and free olefin.[7]

In the course of these studies it became apparent that the stability of the zerovalent metal olefin complexes involved either as final products or reacting substrates was a prime issue in the overall equilibrium and mechanistic pattern, being markedly affected by the nature of both the α-diimine and the olefin.

Recently a study has been published[8a] on the synthesis and reactivity of zerovalent palladium and platinum complexes with olefinic and rigid α-diimine ligands, which showed that back donation of electron density from the metal to the alkene is the major factor determining the stability of these complexes. It was also surmised that substitution of the alkene occurs *via* either associative or dissociative mechanisms, depending on the steric requirements of the α-diimine ligand. However, with the exception of a few NMR equilibrium measurements, no quantitative kinetic data were provided to support these views.

We have now carried out an equilibrium and kinetic study of the olefin substitution in palladium(0) complexes of the type [Pd(η^2-ol)(L–L)] (ol = electron-poor olefin; L–L = 2-NC_5H_4CH=NC_6H_4OMe-4) with the aim of elucidating the influence of the alkene structural factors on the rates and equilibrium constants involved.

Results and Discussion

The system studied is represented in Scheme 1 where the reaction (1) takes place in chloroform under nitrogen. Equilibrium (1) is rapidly established except for ol = dmf or nq, ol′ = tmetc, where the approach to equilibrium can be followed kinetically by UV/VIS spectrophotometric techniques. The course of the reaction was confirmed by direct comparison of the final spectra of reactant mixtures in the range 300–600 nm with those of authentic samples prepared independently. In the cases of ol = dmf, ol′ = an or CH_2=CClCN the products were not isolated owing to the very low equilibrium constant values. However, the spectral changes observed were quite similar to those in the other cases. The equilibrium reactions (1) were also monitored when possible by ^{1}H NMR spectrometry (see below). Again, for ol = dmf, ol′ = an or CH_2=CClCN the unfavourable equilibrium position did not allow detection of the reaction products. Moreover, some decomposition of the complexes to palladium metal took place with time (*ca.* 1 h). A much faster decomposition occurred with ol′ = dimethyl maleate (dmm), which prevented any quantitative measurement also by the UV/VIS spectra.

Determination of equilibrium constants

The equilibrium constants K_e were determined by recording spectral changes in the range 300–600 nm of mixtures obtained by adding appropriate aliquots of solutions of ol′ to a solution of substrate **1** ($[Pd]_{tot}$ *ca.* 1 × 10^{-4} mol dm^{-3}) in the

$$\underset{\mathbf{1}}{[Pd(\eta^2\text{-ol})(L\text{–}L)]} + ol' \overset{K_e}{\rightleftharpoons} \underset{\mathbf{2}}{[Pd(\eta^2\text{-ol}')(L\text{–}L)]} + ol \qquad (1)$$

Scheme 1 L–L = 2-NC_5H_4CH=NC_6H_4OMe-4; ol = dimethyl fumarate (dmf), ol′ = acrylonitrile (an), 1-chloro-1-cyanoethylene (CH_2=CClCN), tetramethyl ethylenetetracarboxylate (tmetc), 1,4-naphthoquinone (nq), fumaronitrile (fn), or maleic anhydride (ma); ol = nq, ol′ = tmetc, fn or ma; ol = fn or ma, ol′ = tetracyanoethylene (tcne)

---

† *Non-SI unit employed:* cal = 4.184 J.

Table 1 Equilibrium constants K_e for reaction (1) in chloroform at 25 °C

ol	ol′	K_e
dmf	an	$(2.1 \pm 0.3) \times 10^{-3}$
	CH_2=CClCN	$(1.0 \pm 0.1) \times 10^{-2}$
	nq	966 ± 46
	tmetc	960 ± 600^{a}
	fn	4400 ± 400
	ma	7900 ± 1900
nq	tmetc	$0.99 \pm 0.6\,(1.2)^{b}$
	fn	3.5 ± 0.2
	ma	7.5 ± 0.6
fn	ma	1.8 ± 0.5^{c}
	tcne	$\longrightarrow \infty$
ma	tcne	$\longrightarrow \infty$

[a] Calculated as K_e(ol = dmf, ol′ = nq)K_e(ol = nq, ol′ = tmetc). [b] Calculated from ^1H NMR spectra in $CDCl_3$ at 25 °C. [c] Calculated as K_e(ol = dmf, ol′ = ma)/K_e(ol = dmf, ol′ = fn).

thermostatted cell compartment of the spectrophotometer. In the cases of high K_e values the equilibrium position was tuned by adding an excess of the olefin being displaced (ol = dmf, ol′ = nq, tmetc, fn or ma).

Abstract factor analysis[9] of the observed spectral changes indicated that at most three independently absorbing species were present, *i.e.* complexes **1** and **2** and nq when involved as either ol or ol′. The absorbance data were fitted by non-linear least squares[10] according to the equations (2)–(6) where D_λ is

$$[\text{ol}][\mathbf{2}]/[\text{ol}'][\mathbf{1}] = K_e \qquad (2)$$

$$[\mathbf{1}] + [\mathbf{2}] = [\text{Pd}]_{\text{tot}} \qquad (3)$$

$$[\text{ol}] + [\text{ol}'] = [\text{ol}]_0 + [\text{ol}']_0 \qquad (4)$$

$$[\text{ol}] = [\text{ol}]_0 + [\mathbf{2}] \qquad (5)$$

$$D_\lambda = \varepsilon_1[\mathbf{1}] + \varepsilon_2[\mathbf{2}] + \varepsilon_{\text{ol}}[\text{ol}] + \varepsilon_{\text{ol}'}[\text{ol}'] \qquad (6)$$

the absorbance. The absorption coefficients ε_{ol} and $\varepsilon_{ol'}$ have negligible values except when ol or ol′ is nq. The parameters to be optimized were K_e and ε_2. When the latter was accessible experimentally from the spectrum of the independently prepared species **2**, it could be held fixed during the iterative fitting process or allowed to float as an optimized parameter. In the latter case the final value turned out to be coincident with that determined directly.

The K_e values at 25 °C are listed in Table 1. The spectral changes for ol = nq and ol′ = fn are shown in Fig. 1. The corresponding fit of the absorbance at 480 nm is shown in Fig. 2. The reaction of tcne with [Pd(η^2-ol)(L–L)] (ol = fn or ma) is shifted completely to the right even in the presence of a large excess of ol, as was already observed with other α-diimine complexes[8a] and no equilibrium constant could be assessed.

The K_e values in Table 1 span a very wide range and appear to increase with increasing electron affinity of the entering activated olefin.[11] Such range is much wider than that observed for the equilibrium constants of reaction (7) as determined by

$$[\text{Ni(ol)L}_2] + \text{ol}' \rightleftharpoons [\text{Ni(ol}')\text{L}_2] + \text{ol} \qquad (7)$$

appropriate combination of the equilibrium constants for reaction (8) (L = phosphorus-donor ligand).[12]

$$[\text{NiL}_3] + \text{ol} \rightleftharpoons [\text{Ni(ol)L}_2] + \text{L} \qquad (8)$$

The very low equilibrium constants for an and CH_2=CClCN complexes are reflected by the inability to isolate zerovalent metal complexes with less electron-poor olefins than dmf [see below and ref. 8(*a*)]. At the other extreme of the stability range we were unable to determine the constant K_e for ol′ = tcne owing to the equilibrium being completely driven to the right. A viable approach to extrapolating its value would be the use of correlations between complex stability and some property of either the free olefins or the palladium(0) olefin complex. Such attempts have already been made.[8a,12–18] However, linear free-energy relationships, although they have become a part of our chemical language, often represent oversimplifications, even more so when effects of diverse nature are involved. In addition, the electronic properties of the olefins result from an interplay of inductive and resonance effects which may be hard to disentangle.[19] Therefore, the usefulness of such relationships is confined within strictly homologous series of compounds.

Within these limitations, the K_e value for ol = dmf, ol′ = tcne can be estimated to be in the order of 10^{16} by correlating log K_e in the series ol = dmf, ol′ = fn, an or tcne to the electron affinities of the olefins as a measure of their electron-accepting abilities.[11]

Our inability to determine K_e for ol = dmf, ol′ = dmm due to rapid decomposition in the reacting mixture reflects the higher kinetic lability of the product [Pd(η^2-dmm)(L–L)]. This

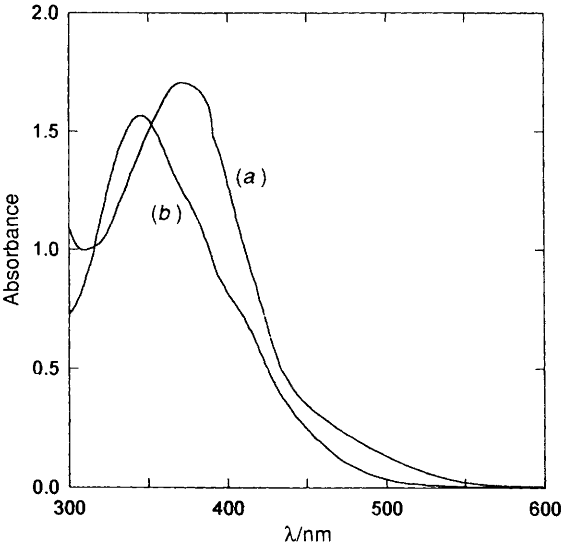

Fig. 1 Spectral changes for equilibrium (1) with ol = nq, ol′ = fn at 25 °C ($[\text{Pd}]_{\text{tot}} = 1 \times 10^{-4}$ mol dm^{-3}): (*a*) [Pd(η^2-nq)(L–L)], (*b*) [Pd(η^2-fn)(L–L)]

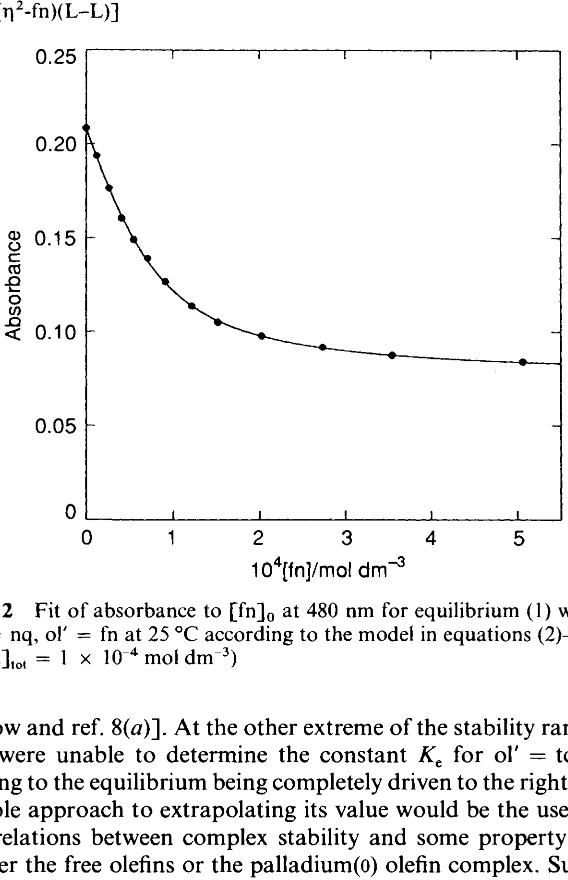

Fig. 2 Fit of absorbance to $[\text{fn}]_0$ at 480 nm for equilibrium (1) with ol = nq, ol′ = fn at 25 °C according to the model in equations (2)–(6) ($[\text{Pd}]_{\text{tot}} = 1 \times 10^{-4}$ mol dm^{-3})

probably results from the lower electron affinity of dmm[16] caused by the removal of conjugation of the C=O and C=C π electrons.[18] In the case of the more sterically crowded olefin tmetc the K_e value was accessible thanks to the presence of four electron-withdrawing groups which apparently offsets the unfavourable steric properties of such olefins. The latter, however, affect appreciably the rate of reaction, as will be shown below.

Determination of rate constants

The rates of approach to equilibrium (1) are in general very high. Only in the cases ol = dmf or nq, ol′ = tmetc the direct and reverse steps were sufficiently slow to be followed by conventional spectrophotometric techniques and a rapid-mixing device.

Reaction (9) was studied by monitoring spectral changes with

$$[\mathrm{Pd}(\eta^2\text{-dmf})(\mathrm{L{-}L})] + \mathrm{tmetc} \underset{k_{-2}}{\overset{k_2}{\rightleftharpoons}} [\mathrm{Pd}(\eta^2\text{-tmetc})(\mathrm{L{-}L})] + \mathrm{dmf} \quad (9)$$

time in the range 300–420 nm in the presence of a constant ten-fold excess of dmf over the metal substrate ($[\mathrm{Pd}]_0 = 5 \times 10^{-5}$ mol dm^{-3}) and of tmetc in the concentration range 5×10^{-4}–5×10^{-3} mol dm^{-3}. Under these conditions the disappearance of the starting metal complex followed the rate law (10) with a

$$-\mathrm{d}[\mathrm{Pd}(\eta^2\text{-dmf})(\mathrm{L{-}L})]/\mathrm{d}t = k_2[\mathrm{tmetc}][\mathrm{Pd}(\eta^2\text{-dmf})(\mathrm{L{-}L})] - k_{-2}[\mathrm{dmf}][\mathrm{Pd}(\eta^2\text{-tmetc})(\mathrm{L{-}L})] \quad (10)$$

pseudo-first-order rate constant k_{obs} given by (11), as expected

$$k_{\mathrm{obs}} = k_2[\mathrm{tmetc}] + k_{-2}[\mathrm{dmf}] \quad (11)$$

for an approach to equilibrium *via* direct and reverse first-order steps.[20] However, owing to the high equilibrium constant of the system and the attendant low value of k_{-2}, only the k_2 term could be determined with sufficient accuracy by linear regression according to equation (11). The k_2 values at temperatures in the range 15–40 °C are listed in Table 2, activation parameters in Table 4.

The comparatively low activation enthalpy and the highly negative activation entropy are in agreement with an associative mechanism in which both the entering and the leaving olefins are present in the 18-electron transition state of an activation process involving considerable freezing of degrees of freedom. Similar results were obtained for the exchange of activated olefins in palladium(0) phosphine complexes.[16] An associative process was also proposed for olefin exchange in rigid α-diimine complexes.[8a]

Table 2 Second-order rate constants k_2, for the reaction $[\mathrm{Pd}(\eta^2\text{-dmf})(\mathrm{L{-}L})] + \mathrm{tmetc} \longrightarrow [\mathrm{Pd}(\eta^2\text{-tmetc})(\mathrm{L{-}L})] + \mathrm{dmf}$ in $CHCl_3$

T/°C	k_2/dm^3 mol^{-1} s^{-1}
15	1.16 ± 0.05
25	1.81 ± 0.06
32	2.12 ± 0.06
40	2.98 ± 0.09

Table 3 Second-order rate constants for the forward (k_2) and reverse (k_{-2}) steps of the reaction $[\mathrm{Pd}(\eta^2\text{-nq})(\mathrm{L{-}L})] + \mathrm{tmetc} \rightleftharpoons [\mathrm{Pd}(\eta^2\text{-tmetc})(\mathrm{L{-}L})] + \mathrm{nq}$ in $CHCl_3$

T/°C	k_2/dm^3 mol^{-1} s^{-1}	k_{-2}/dm^3 mol^{-1} s^{-1}	K_e*
15	8.6 ± 0.2	6.8 ± 0.9	1.26 ± 0.2
25	13.9 ± 0.8	14 ± 1	0.96 ± 0.1
32	24 ± 1	28 ± 4	0.86 ± 0.1
40	35 ± 2	45 ± 6	0.78 ± 0.1

* Calculated as k_2/k_{-2}.

In the case of reaction (12) the much more balanced

$$\underset{\mathbf{A}}{[\mathrm{Pd}(\eta^2\text{-nq})(\mathrm{L{-}L})]} + \underset{\mathbf{B}}{\mathrm{tmetc}} \underset{k_{-2}}{\overset{k_2}{\rightleftharpoons}} \underset{\mathbf{C}}{[\mathrm{Pd}(\eta^2\text{-tmetc})(\mathrm{L{-}L})]} + \underset{\mathbf{D}}{\mathrm{nq}} \quad (12)$$

equilibrium position (Table 1) allowed the system to be studied under second-order conditions in both directions. Absorbance data D_t were then fitted with time according to model (13)

$$-\mathrm{d}[\mathbf{A}]/\mathrm{d}t = k_2[\mathbf{A}]([\mathbf{B}]_0 - [\mathbf{A}]_0 + [\mathbf{A}]) - k_{-2}([\mathbf{A}]_0 - [\mathbf{A}])^2 \quad (13)$$

for second-order reversible reactions,[20] where $[\mathbf{A}]_0$ and $[\mathbf{B}]_0$ are initial concentrations (1×10^{-4} and in the range 1×10^{-4}–5×10^{-4} mol dm^{-3}, respectively) and $[\mathbf{C}] = [\mathbf{D}] = [\mathbf{A}]_0 - [\mathbf{A}]$. Integration of equation (13) yields expression (14) where

$$[\mathbf{A}] = A_{\mathrm{eq}} - [Q/(1 - E)] \quad (14)$$

$Q = \{K_e^2([\mathbf{B}]_0 - [\mathbf{A}]_0)^2 + 4[\mathbf{A}]_0[\mathbf{B}]_0K_e\}^{\frac{1}{2}}/(K_e - 1)$, $K_e = k_2/k_{-2}$, $A_{\mathrm{eq}} = \{Q(K_e - 1) - K_e([\mathbf{B}]_0 - [\mathbf{A}]_0) + 2[\mathbf{A}]_0)\}/2(K_e - 1)$, $E = ([\mathbf{A}]_0 - A_{\mathrm{eq}} + Q)\exp[(k_2 - k_{-2})Qt]/([\mathbf{A}]_0 - A_{\mathrm{eq}})$, A_{eq} is the equilibrium concentration of **A** and t is the time. The absorbance D_t will be given by equation (15). Non-linear regression of D_t with time using k_2, k_{-2},

$$D_t = \varepsilon_A[\mathbf{A}] + \varepsilon_C[\mathbf{C}] + \varepsilon_D[\mathbf{D}] = \varepsilon_A[\mathbf{A}] + [\mathbf{C}](\varepsilon_C + \varepsilon_D) \quad (15)$$

$\varepsilon_C + \varepsilon_D$ as the parameters to be optimized[10] gave the data listed in (Table 3) in the temperature range 15–40 °C (Fig. 3). The resulting absorption coefficients at 380 nm were in excellent agreement with those determined independently from the Beer–Lambert law applied to solutions of pure **C** or **D**.

Alternatively, the k_2 and k_{-2} values for reactions at selected temperatures (15 and 32 °C) were measured directly under pseudo-first-order conditions starting from either **A** or **C** in the presence of a large excess of the entering olefin **B** or **D**, respectively, as the slopes of plots of expressions (16) or (17).

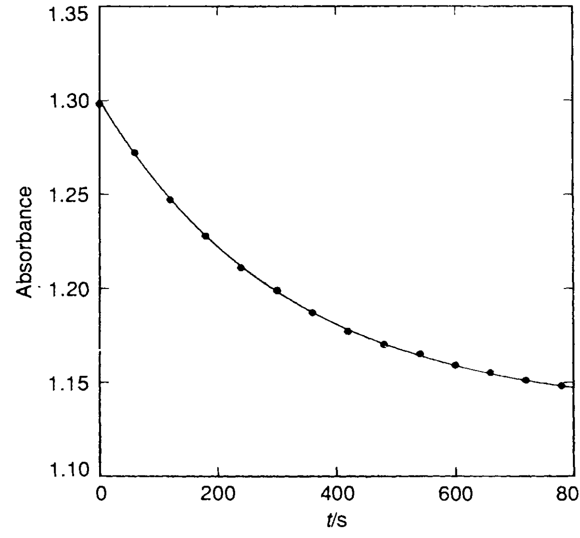

Fig. 3 Fit of absorbance to time for reaction (12) according to the integrated form of rate law (13) [equation (14)] at 25 °C and 380 nm ($[\mathrm{Pd}]_{\mathrm{tot}} = 1 \times 10^{-4}$, $[\mathrm{tmetc}]_0 = 1.25 \times 10^{-4}$ mol dm^{-3})

$$k_{obs} = k_2[\mathbf{B}] \tag{16}$$

$$k'_{obs} = k_{-2}[\mathbf{D}] \tag{17}$$

Under these conditions the equilibrium conversion in either sense was more than 90%.

The two sets of rate constants derived from these alternative methods were in very good agreement, showing the internal consistency of the treatment. Moreover, the ratio k_2/k_{-2} 0.96 ± 0.08 at 25 °C was virtually identical to the equilibrium constant K_e directly determined earlier for reaction (12) (Table 1), though being affected by a much lower uncertainty. Consistently, the equilibrium constants at the other temperatures examined were calculated as the ratios k_2/k_{-2} since their measurement by spectrophotometric methods was affected by large errors and the K_e values depend only slightly on temperature.

Activation parameters for both k_2 and k_{-2} paths of reaction (12) are listed in Table 4. It appears that also for reaction (12) the direct and reverse steps are associative in nature. The higher negative activation entropy for the entry of tmetc relative to its release in the reverse reaction is probably ascribed to the decrease in the degrees of freedom of the CO_2Me substituents in this olefin during the k_2 activation process. The reverse k_{-2} step is likely to involve some balance between the negative entropy typical of an associative process and the removal of constraints due to the release of tmetc as compared to the more rigid nq moiety. On the other hand, the k_2 step appears to be slightly favoured from the enthalpy point of view, reflecting the higher stability of the tmetc metal complex over its nq counterpart as related to the higher electron-withdrawing ability of tmetc. The interplay of these enthalpy/entropy factors results in an equilibrium constant near unity for the global reaction (12) (see also ΔH° and ΔS° values in Table 4).

The much lower rate of displacement of dmf as compared to nq (*cf.* Tables 2–4) arises from the much more negative activation entropy for the direct k_2 step of reaction (9) which offsets the more favourable activation enthalpy.

Proton NMR investigations

The solution behaviour of complexes [Pd(η^2-olefin)(L–L)] is conveniently studied by ^1H NMR spectroscopy.[3,8a] Thus, the establishment of equilibrium (1) was generally monitored for [Pd(η^2-ol)(L–L)]–ol′ mixtures (1 : 1 molar ratio) in $CDCl_3$ at 25 °C, with initial concentrations of the starting complex ranging from 2×10^{-3} to 4×10^{-3} mol dm^{-3}. In the spectra of the equilibrium system ol = nq, ol′ = tmetc, for which the K_e value is *ca.* 1, the typical α-diimine signals of both [Pd(η^2-ol)(L–L)] and [Pd(η^2-ol′)(L–L)] species are observed. Integration of the 2-pyridyl H(6) and/or the imino N=CH proton resonances yields an equilibrium constant K_e in good agreement with that measured by the UV/VIS technique (Table 1).

In the presence of free olefin the complexes [Pd(η^2-ol)(L–L)] undergo rapid exchange (on the NMR time-scale) between free and co-ordinated olefin, when the alkene is dmf, nq or fn. The rate of such exchange, however, is dramatically reduced when the bulkier tmetc ligand is involved, other things being equal. In fact, the ^1H NMR spectrum of [Pd(η^2-tmetc)(L–L)]–tmetc mixtures (1 : 0.5–1 molar ratio) in $CDCl_3$ at 25 °C shows a sharp singlet at δ 3.87 for the OMe protons of the free olefin and two 1 : 1 sharp singlets at δ 3.74 and 3.63 for the corresponding protons of the ligand. The retarding effect of increasing steric requirements around the metal centre on the rates of olefin substitution and olefin exchange has been previously observed for related complexes [Pd(η^2-ol)(L–L)], where L–L is a rigid bidentate α-diimine ligand,[8a] in agreement with an essentially associative mechanism analogous to that proposed for reactions (9) and (12) involving tmetc as entering or leaving alkene (see earlier).

Table 4 Activation and thermodynamic parameters for the reaction [Pd(η^2-ol)(L–L)] + tmetc $\rightleftharpoons$ [Pd(η^2-tmetc)(L–L)] + ol in $CHCl_3$

Olefin, ol	$\Delta H_2^\ddagger$/ Kcal mol^{-1}	$\Delta S_2^\ddagger$/ cal K^{-1} mol^{-1}	$\Delta H_{-2}^\ddagger$/ Kcal mol^{-1}	$\Delta S_{-2}^\ddagger$/ cal K^{-1} mol^{-1}
nq	9.7 ± 0.7	−20 ± 2	13.2 ± 0.8	−9 ± 2
$\Delta H^{\circ a} = -3.5 \pm 0.5$ kcal mol^{-1}, $\Delta S^{\circ b} = -11 \pm 2$ cal K^{-1} mol^{-1}				
dmf	6.2 ± 0.5	−36 ± 2		

[a] Calculated as $\Delta H_2^\ddagger - \Delta H_{-2}^\ddagger$. [b] Calculated as $\Delta S_2^\ddagger - \Delta S_{-2}^\ddagger$.

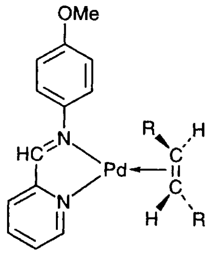

I

As previously reported,[3] the complex [Pd(η^2-dmf)(L–L)] is stereochemically non-rigid in solution. In the ^1H NMR spectrum the olefinic OMe protons are detected as a singlet (δ 3.62 in $CDCl_3$ at 25 °C) even at the lowest temperature explored (−60 °C), despite the asymmetric nature of the α-diimine moiety in a compound of type I (R = CO_2Me). For the complex [Pd(η^2-ol)(L–L)] a trigonal-planar co-ordination around the Pd with the olefin plane nearly perpendicular to the Pd(L–L) plane is assumed in accordance with what is generally found in three-co-ordinate d^{10} derivatives [M(η^2-ol)L_2] (M = Pd or Pt).[8b] When L_2 is a rigid bidentate α-diimine ligand and M = Pd the above structure has been confirmed by an X-ray structural investigation.[8a] In contrast, the complex [Pd(η^2-tmetc)(L–L)] containing a bulkier and more π-accepting olefin shows no fluxional behaviour even at the highest temperature studied (55 °C), as suggested by the appearance of two sharp 1 : 1 singlets for the OMe olefinic protons in the ^1H NMR $CDCl_3$ spectra at any temperature.

In the case of [Pd(η^2-fn)(L–L)] the olefinic protons appear as an AB quartet centred at δ 3.02 (J_{AB} = 8.8 Hz) in $CDCl_3$ at 25 °C, which coalesces into a broad singlet when the temperature is raised to 50 °C. These findings are better interpreted on the basis of a dynamic process involving rotation of the co-ordinated olefin around the metal–olefin bond axis, with a rotational barrier increasing with increasing π-accepting properties and steric requirements of the olefin. The $\Delta G_{rot}^\ddagger$ value of 70.0 kJ mol^{-1}, computed from the coalescence temperature and the value of 15.4 Hz for $\nu_A - \nu_B$ of [Pd(η^2-fn)(L–L)], is similar to those reported for olefin rotation in analogous palladium(0) olefin complexes with rigid α-diimine ligands (50–69 kJ mol^{-1}).[8] On the other hand, mechanisms such as Pd–N bond breaking/making or palladium–olefin dissociation–association, would hardly explain the rigid behaviour of the more sterically hindered [Pd(η^2-tmetc)(L–L)] derivative.

Experimental

Preparation of complexes

The complexes [Pd(η^2-ol)(L–L)] (ol = dmf, fn, ma or nq) and the olefin tmetc were prepared according to published procedures.[3,21] The complexes [Pd(η^2-ol)(L–L)] (ol = fn, ma, nq, tmetc or tcne) can also be prepared by olefin displacement from [Pd(η^2-dmf)(L–L)] as described below for ol = fn.

Table 5 Analytical, selected IR and ^1H NMR data for new complexes $[Pd(\eta^2\text{-ol})(L\text{–}L)]$

	ol = tmetc			ol = tcne		
	C	H	N	C	H	N
Elemental analysis[a] (%)	47.8	4.1	4.8	51.2	2.7	18.7
	(47.7)	(4.2)	(4.85)	(51.1)	(2.7)	(18.8)
IR[b]						
ν(C=N)	1613m			1618m		
ν(C≡N)				2227s		
ν(C=O)	1731s, 1710s, 1687s					
^1H NMR[c] (δ)						
N=CH	8.57 (s)			8.57 (s)		
Pyridyl protons						
H^3	7.73 (m)			7.94 (m)		
H^4	7.90 (m)			8.10 (m)		
H^5	7.52 (m)			7.77 (m)		
H^6	9.01 (m)			8.91 (m)		
$C_6H_4OCH_3$	3.85 (s)			3.90 (s)		
$OCOCH_3$	3.74 (s), 3.63 (s)					

[a] Calculated values in parentheses. [b] As Nujol mulls; m = medium, s = strong. [c] Recorded at 200.132 MHz in $CDCl_3$ at 25 °C; m = multiplet, s = singlet.

To a solution of $[Pd(\eta^2\text{-dmf})(L\text{–}L)]$ (0.40g, 1.01 mmol) in CH_2Cl_2 (100 cm^3) was added fn (0.095g, 1.21 mmol) dissolved in the minimum volume of CH_2Cl_2 (30 cm^3). The solution was stirred for 30 min and then reduced to small volume on a rotary evaporator. A small amount of activated carbon was added and the resulting mixture filtered on a Celite filter. Addition of diethyl ether yielded $[Pd(\eta^2\text{-fn})(L\text{–}L)]$ as a yellow precipitate which was filtered off, washed repeatedly with diethyl ether, and dried *in vacuo* at 40 °C (0.36 g, yield 94%).

The complex $[Pd(\eta^2\text{-tmetc})(L\text{–}L)]$ required a longer reaction time (24 h). The complex with tcne can also be prepared from $[Pd(\eta^2\text{-olefin})(L\text{–}L)]$ (olefin = nq, fn or ma) following the above procedure.

All reactions were carried out under a nitrogen atmosphere at room temperature. Analytical, IR and ^1H NMR data for the new complexes (olefin = tmetc or tcne) are listed in Table 5.

The solvent $CHCl_3$ was purified by washing with water, drying over anhydrous calcium chloride and distillation; $CDCl_3$ was treated with anhydrous sodium carbonate before use.

Equilibrium measurements

The setting up of equilibrium mixtures was carried out under a dry nitrogen atmosphere by means of a laboratory-made dry-box. The silica glass cells were sealed within the dry-box and then transferred to the thermostatted cell compartment of the spectrophotometer. The spectra were recorded after thermal equilibration. Freshly prepared solutions of the complexes were used in order to avoid decomposition effects.

Kinetic measurements

Prethermostatted kinetic solutions previously stored under dry nitrogen were mixed directly in the cell compartment by means of Gilson micropipettes or by using a Hi-Tech SFA II rapid kinetic accessory for the faster reactions ($t_{\frac{1}{2}} < 20$ s). Absorbance readings were taken at selected times either at fixed wavelength (490 or 380 nm) for the faster reactions or by repetitive scanning in the range 300–420 nm.

Apparatus and instrumentation

The UV/VIS spectra were recorded on a Perkin-Elmer Lambda 5 instrument equipped with a Peltier effect (Perkin-Elmer) thermostatting apparatus, IR spectra on Nicolet 750 or Bio-Rad FTR 40 spectrophotometers and ^1H NMR spectra on a Bruker AC 200 spectrometer.

Data analysis

Mathematical and statistical analysis of equilibrium and kinetic data was carried out on a personal computer equipped with an INTEL 486 66 MHz CPU by the use of a locally adapted version of Marquardt's non-linear regression algorithm[10] written in TURBOBASIC™ (Borland). Abstract factor analysis was carried out in the MATLAB™ (Mathworks) environment.

Acknowledgements

Financial support by the Italian Ministero dell'Universitá e della Ricerca Scientifica e Tecnologica (Research Funds 40 and 60%) is gratefully acknowledged.

References

1 J. Reinhold, R. Benedix, P. Birner and H. Hennig, *Inorg. Chim. Acta.*, 1979, **33**, 209; H. van der Poel and G. van Koten, *Inorg. Chem.*, 1981, **20**, 2950; H. van der Poel, G. van Koten and G. C. van Stein, *J. Chem. Soc., Dalton Trans.*, 1981, 2164; M. E. Cucciolito, V. De Felice, A. Panunzi and A. Vitagliano, *Organometallics*, 1989, **8**, 1180.

2 B. Crociani, F. Di Bianca, R. Bertani and C. Bisi-Castellani, *Inorg. Chim. Acta*, 1985, **101**, 161; R. Bertani, A. Berton, F. Di Bianca and B. Crociani, *J. Organomet. Chem.*, 1986, **303**, 283.

3 B. Crociani, F. Di Bianca, P. Uguagliati, L. Canovese and A. Berton *J. Chem. Soc., Dalton Trans.*, 1991, 71.

4 B. Crociani, S. Antonaroli, F. Di Bianca, L. Canovese, F. Visentin and P. Uguagliati, *J. Chem. Soc., Dalton Trans.*, 1994, 1145.

5 L. Canovese, F. Visentin, P. Uguagliati, F. Di Bianca, S. Antonaroli and B. Crociani, *J. Chem. Soc., Dalton Trans.*, 1994, 3113.

6 L. Canovese, F. Visentin, P. Uguagliati, B. Crociani and F. Di Bianca, *Inorg. Chim. Acta*, 1995, **235**, 45.

7 L. Canovese, F. Visentin, P. Uguagliati, F. Di Bianca, A. Fontana and B. Crociani, *J. Organomet. Chem.*, 1996, **508**, 101.

8 (*a*) R. van Asselt, C. J. Elsevier, W. J. J. Smeets and A. L. Spek, *Inorg. Chem.*, 1994, **33**, 1521; (*b*) S. D. Ittel and J. A. Ibers, *Adv. Organomet. Chem.*, 1976, **14**, 33; K. J. Cavell, D. J. Stufkens and K. Vrieze, *Inorg. Chim. Acta*, 1981, **47**, 67.

9 P. Uguagliati, A. Benedetti, S. Enzo and L. Schiffini, *Comput. Chem.*, 1984, **8**, 161.

10 D. W. Marquardt, *SIAM J. Appl. Math.*, 1963, **11**, 431.

11 J. K. Kochi, *Organometallic Mechanisms and Catalysis*, Academic Press, New York, 1978, ch. 17, Table II and refs. therein.

12 C. A. Tolman, *J. Am. Chem. Soc.*, 1974, **96**, 2780.

13 S. Cenini, R. Ugo and G. La Monica, *J. Chem. Soc. A*, 1971, 409.

14 H. Minematsu, Y. Nonaka, S. Takahashi and N. Hagihara, *J. Organomet. Chem.*, 1973, **59**, 395.

15 Ts. Ito, S. Hasegawa, Y. Takahashi and Y. Ishii, *J. Organomet. Chem.*, 1974, **73**, 401.
16 F. Ozawa, T. Ito, Y. Nakamura and A. Yamamoto, *J. Organomet. Chem.*, 1979, **168**, 375.
17 N. Ito, T. Saji and S. Aoyagui, *Bull. Chem. Soc. Jpn.*, 1985, **58**, 2323.
18 G. Pellizer, M. Lenarda, R. Ganzerla and M. Graziani, *Gazz. Chim. Ital.*, 1986, **116**, 155.
19 S. D. Ittel, *Inorg. Chem.*, 1977, **16**, 2589.
20 A. A. Frost and R. G. Pearson, *Kinetics and Mechanism*, 2nd edn., Wiley, New York, 1961, ch. 8.
21 H. K. Hall, jun., and R. C. Daly, *Macromolecules*, 1975, **8**, 22 and refs. therein.

Received 20*th September* 1995; *Paper* 5/06208J